Fracture of a Thin Laminated Foil

Ståhle, P.; Andreasson, E.; Kao-Walter, S.

Published in:
Procedia Materials Science

2014

Document Version:
Publisher's PDF, also known as Version of record

Available online at www.sciencedirect.com

SciVerse ScienceDirect

Procedia Materials Science 00 (2014) 000–000

Procedia Materials Science

www.elsevier.com/locate/procedia

20th European Conference on Fracture (ECF20)

Fracture of a thin laminated foil

Per Ståhle[a,*], Eskil Andreasson[b,c], Sharon Kao-Walter[c]

[a]*Lund University, Ole Römers väg, SE-221 00 Lund, Sweden*
[b]*Tetra Pak Packaging Solutions, Ruben Rausings gata, SE-221 86 Lund, Sweden*
[c]*Dept. of Mech. Eng. School of Eng., Blekinge Institute of Technology, SE-371 79 Karlskrona, Sweden*

Abstract

The micro-mechanisms of fracture in a laminate composed of an aluminium foil and a polyethene film are considered. The laminate as well as the freestanding layers were fracture mechanically tested. Inspection of the broken cross-sections shows that fracture occurs through necking, i.e., localised plastic deformation leading to a decreasing and eventually vanishing cross-section. This occurs ahead of the crack tip for both freestanding layers and the laminate. The plastic properties and a slip-line theory are successfully used to derive the work of failure. An accurate prediction of the fracture toughness is made for the aluminium foil and the laminate. Even though the toughness of the freestanding polyethene film could not be accurately determined by the theory, its role as a member of the laminate is predicted by the theory with great accuracy. It is shown that the load carrying capacity of the laminate is many times larger than the added load carried by the freestanding layers. The study further indicates that necking may be impeded which may increase the toughness several times. It is also shown how the laminate may be forced to produce multiple necking with a significantly improved toughness as a result.

Selection and peer-review under responsibility of the Norwegian University of Science and Technology (NTNU), Department of Structural Engineering.

Keywords: Type your keywords here, separated by semicolons;

1. Introduction

An aluminium foil (Al-foil) and a low-density polyethylene (LDPF) polymer film, that are studied in this work, are widely used in aseptic food packages. The immediate industrial applications of the obtained results are development of new packaging material concerning opening devices and oxygen barriers.

The Al-foil is used as an efficient barrier towards exposure to oxygen and light in food packages. In liquid containers the Al-foil is usually coated with a ductile polymer layer to prevent leakage. Layers of paperboard are also often added to improve the mechanical properties of the structure. The packaging materials are exposed to different loading conditions during their lifetime; forming, folding, filling, distribution, storage, handling and finally opening, wasting and recycling. In liquid containers a difficulty, typically during forming and folding, is to avoid that cracks initiate in the Al-foil layer, that cannot withstand as high local strains as the polymer and the paper layers. Occasionally, these

* Corresponding author. Tel.: +0-000-000-0000 ; fax: +0-000-000-0000.
E-mail address: author@institute.xxx

2211-8128
Selection and peer-review under responsibility of the Norwegian University of Science and Technology (NTNU), Department of Structural Engineering.

cracks grow and the function of the barrier eventually becomes insufficient. Cracks initiated in the Al-foil can eventually spread into the polymer and the paper layers. It is, therefore, important to understand the individual fracture behaviour of the Al-foil and the LDPE layers and their roles as a member of the laminated structure.

Nomenclature

A radius of
B position of
C further nomenclature continues down the page inside the text box

Opening devices is another important application, which in recent years has significantly increased in volume in the packaging industry. The failure process in the opening application is intended, therefore the initiation and propagation of the process leading to completed fracture has to be controlled. Observations show that the mechanisms of failure are similar in both opening devices and the functionality of barrier in liquid packages **?**.

Commonly a packaging material consists of several material layers; paperboard, LDPE and Al-foil. In this work the focus is solely on Al-foil and the LDPE layers. The paperboard layer is excluded in this particular study. To predict the fracture in the laminate, the fracture behaviour of the Al-foil and the polymer are at first studied separately. Several studies of the fracture behaviour of the individual packaging material layers, for example paperboard, are presented in **?**-**?** and a metal film on a polymer substrate used in flexible electronics applications **?**-**?**. To form a well defined basis for the investigation of Al-foil and LDPE, centre-cracked panels exposed to in-plane uni-axial tensile mode I loading are further analysed in this work. Adhesion between the different material layers has in this study been simplified and idealized. The chemical bonds between the different layers are assigned similar strength as the induced traction forces created when the individual material layers contract due to localization, thus leading to separation of the material layers locally. Delamination and the level of adhesion is an intriguing topic **?**-**?** and has to be included in future works.

Micro-mechanical understanding of the local plastic effects involved in the fracture processes are in focus. This knowledge is necessary to make appropriate assumptions and to create accurate and reliable computer simulation models of the described events on a macroscopic scale. Selection of appropriate constitutive models for the continuum material and how the crack initiates and propagates to various loading conditions can also be simplified. Hardware and software improvements have emerged during the last decades. Therefore the demand has significantly increased during the last years to provide efficient and sufficiently simple tools to solve industrial applications where failure initiation and subsequent crack growth need to be accurately predicted. As it was pointed out in **?**, mechanical modeling of the polymer material in study is still in a rather early stage. A cell model has been so far developed and applied to investigate the effect of voids on matrix yielding and localized plastic deformation **?**-**?**. In the present work, a modified Dugdale model based on the slip-lines that were observed on specimens cross-section was applied. This approach was utilized to study the localized plastic deformation of the single layer as well as the laminate. The fracture behavior of the Al-foil and LDPE laminate has also been studied in previous work **?**-**?**. A frequent observation is the large variety of failure mechanisms in laminates of different compositions. Furthermore, crack tip fields for stationary and propagating cracks have been investigated. Furthermore, the crack tip fields and crack propagation as well as toughening mechanisms in a process zone of a laminate with a stationary crack tip have been investigated in **?**.

The aim of this work is to present results of the mechanical response of the two materials that may be incorporated in virtual material models for prediction of the different package functionalities. The aim is that the presented approaches should be possible to incorporate and to be utilize as an efficient and powerful tool for solving industrial engineering problems.

In section 2 the material properties are given. Section 3 describes the experimental set-up and experimental results. Sections 4 and 5 describe the capturing of a scanning electron microscope (SEM) images, results and the post test observations. Section 6 describes the equations of the micro-mechanical processes using a slip-line theory and in section 7 linear fracture mechanics and a strip yield model of Dugdale-Barenblatt type are used to compute the mechanical behaviour of the macroscopic crack. Also here the analytical models are used to examine the experimental data.

The model corresponds to the following elastic problem: A linear elastic semi-infinite body, occupying the upper half plane $y > 0$, is subject to the remote stress troo and the following boundary conditions on $y = 0$,

$$\begin{array}{rl} \tau_{xy} = 0 & \\ \sigma_y = 0 & for \quad |x| < a_o \\ \sigma_y = \sigma_y(v) & for \;\; a_o \le |x| < a \;\; and \\ v = 0 & for \quad a \le |x| \;\; . \end{array} \tag{1}$$

The Muskhelishvili [X] complex potentials $\Phi(z)$ and $\psi(z)$ are used, where $z = x + iy$. By defining $\Phi(z)$ as $\bar{\Phi}(z) + z\bar{\Phi}'(z) + \bar{\psi}(z)$ in y ¡ 0, one may eliminate $\psi(z)$ to obtain

$$\sigma_x + \sigma_y = 2\left[\Phi(z) + \bar{\Phi}(z)\right] , \tag{2}$$

$$\sigma_y - i\tau_{xy} = \Phi(z) + \Phi(\bar{z}) + (z - \bar{z})\bar{\Phi}'(\bar{z}) , \tag{3}$$

and

$$2\mu\left[u'(z) + iv'(z)\right] = \kappa\Phi(z) - \Phi(\bar{z}) - (z - \bar{z})\bar{\Phi}'(\bar{z}) , \tag{4}$$

where $\mu = E/\left[2(1 + \nu)\right]$ and $\kappa = (3 - \nu)/(1 + \nu)$ for plane stress.

Along the x-axis (3) and (4) will, due to the symmetry of τ_{xy} and u with respect to the line $y = 0$, give

$$\sigma_y = \Phi_+ + \Phi_- \tag{5}$$

and

$$\frac{\partial v}{\partial x} = \frac{2}{iE}\left(\Phi_+ - \Phi_-\right) , \tag{6}$$

where

$$\Phi_\pm(x) = y \to 0 \lim \Phi(x \pm iy) \quad y > 0 . \tag{7}$$

Thus the boundary conditions can be written on the form

$$\Phi_+(t) + G(t)\Phi_-(t) = f(t) , \tag{8}$$

where

$$G(t) = \begin{cases} 1 & for \;\; |t| < a , \\ -1 & for \;\; a \le |t| \end{cases} \tag{9}$$

and

$$f(t) = \begin{cases} \sigma_y(t) & for \qquad a_o < |t| < a , \\ 0 & for \;\; a_o < |t| \le a_o \; and \; a \le |t| \;\; . \end{cases} \tag{10}$$

The solution (cf. Muskhelishvili [X]) is

$$\Phi(z) = \frac{i}{\pi} z\sqrt{z^2 - a^2}\int_{a_o}^{a} \sigma_y(t)\frac{\sqrt{t^2 - a^2}}{z^2 - t^2}dt + \frac{p(z)}{\sqrt{z^2 - a^2}} , \tag{11}$$

where $p(z)$ can, on account of the symmetry and by letting $z \to \infty$ be identified as $\sigma_\infty z/2$. The assumption that the stresses should remain bounded everywhere implies that

$$\sigma_\infty = \frac{2}{\pi}\int_{a_o}^{a} \sigma_y(t)\frac{dt}{\sqrt{a^2 - t^2}} \;\; . \tag{12}$$

Letting $y \to 0$ using (6), (11) and (12) give

$$\frac{\partial v}{\partial x} = \frac{4}{\pi E} \frac{x}{\sqrt{a^2 - x^2}} \int_{a_o}^{a} \sigma_y(t) \left(\frac{\sqrt{a^2 - t^2}}{x^2 - t^2} - \frac{1}{\sqrt{a^2 - t^2}} \right) dt \, . \tag{13}$$

After integration (13) reads

$$v(x) = \frac{2}{\pi E} \int_{a_o}^{a} \sigma_y(t) \left(\ln \left[\sqrt{a^2 - x^2} + \sqrt{a^2 - t^2} \right] - \ln \left| \sqrt{a^2 - x^2} - \sqrt{a^2 - t^2} \right| - 2 \sqrt{\frac{a^2 - x^2}{a^2 - t^2}} \right) dt \tag{14}$$

In the it is assumed that σ_y is a function of the displacements v. Knowledge of this function enables calculation of relations between σ_y and x for the process region. Reversly, given a stress distribution with respect to x, the resulting σ_y vs. v relationship can be calculated. The relation between stress and displacement is given by

$$\sigma_y(x) = \sigma_D (1 - \frac{x - a}{a_o - a} \frac{v_o}{h}) \tag{15}$$

2. Materials

A $9.0 \mu m$ thick, fully annealed AA1200 Al-foil and a $27.0 \mu m$ thick LDPE polymer film with the product name LD270 are studied.

To simplify the analyses both materials are treated as homogeneous and isotropic elastic plastic. The following properties have been measured for the studied Al-foil, A is used as an index referring to Al-foil: modulus of elasticity $E_A = 55.6 GPa$ and ultimate tensile stress is $\sigma_{bA} = 74 \; MPa$. The yield stress is not easily determined. The lowest possible stress at which plastic deformation occurs is estimated to be at $\sigma_{YA} = 36.2 MPa$ **?**. The elastic modulus is low as compared to what is expected for the bulk material. A large variety of studies using direct tensile testing of thin foils, optical methods for measuring displacements, indentation tests etc. obtain a large variation of moduli ranging from $25 GPa$ to slightly above $70 GPa$ **?**-**?**. The value chosen is obtained at the present experiments for the studied Al-foil . It may be noted that the elastic moduli has little effect on the resulting toughness whereas the fracture process is essentially large plastic straining. For the LDPE, denoted with a index L, the modulus of elasticity is measured to be E_L= $126 MPa$ with the ultimate tensile stress $\sigma_{bL} = 8 MPa$ The yield stress is estimated to $\sigma_{YL} = 5.3 MPa$ which is in accordance with the result **?**. Poisson's ratio is not easily measured. Commonly used are values around 0.3 as for many metals. In **?** $\nu_A = 0.33$ is used for Al-foil and LDPE is known to be close to incompressible with very high Poisson's ratios, e.g. in **?** $\nu_L = 0.45$. As opposed to this **?** use $\nu = 0.3$ for a laminate where the contraction is dominated by the LDPE. Since the laminate is composed of around 10% Al-foil and the rest is LDPE the conclusion is that Poisson's ratio is selected to $\nu_L = 0.3$ for the LDPE.

3. Tensile tests of centre-cracked specimens

Thin centre-cracked sheets, as shown in the fracture mechanical experimental set-up in Fig. **??**, were used for evaluating the toughness of the laminate, i.e. the polymer-coated sheet and the individual material layers of Al-foil and LDPE. Testing was performed according to the ASTM (D-882-91) convention **?**.

Pre-fabricated cracks were manually cut, using a sharp scalpel, with crack lengths ranging from $2a = 2mm$ to $45mm$. The width and gauge length of the specimens was $2W = 95mm$ and $2H = 230mm$, respectively. A pair of wide clamps was used as shown in Fig. **??**. The experimental tests were made at room temperature in an MTS Universal Testing Machine in the Laboratory facilities at Blekinge Institute of Technology. The upper clamp is attached to a $2.5kN$ load cell. The slightly oversized load cell was needed because of the rather heavy clamps. After positioning the specimen, the upper and lower clamps are closed and pressure was applied to tighten four equally spaced quick-acting locking nuts along the front of each clamp. Specimens were extended by traversing the upper cross-head at a constant speed of 7 mm/min. The software TestWorks was used to control the load frame and also to record test data. During testing, the position of the cross-heads and the applied load was monitored and recorded. The tests of the laminates

were run until the entire cross-section was fractured. Experimental results from the individual material layers, Al-foil and, are shown in Figs. **??** a) and b).

Noticeable for the material tests without a centre-crack, describing the continuum behaviour, is the observation that the load after reaching its maximum load decreases in a controlled way. This seems to be due to the structural softening that is initiated at imperfections. The source of the imperfections may be inhomogeneities occurring when cutting the specimens or voids and inclusions present in the raw-material, created in the handling or during the fabrication, which leads to large scattering of the maximum elongation of the latter part in the un-notched specimens. Averaged results from five tests of each case are presented in both graphs. The tensile strength systematically decreases with increasing crack lengths. Implementing a centre-crack in the specimen enables repeatable results for the controlled fracture mechanical testing.

The results from the one-side laminated Al-foil with LDPE and a summary of the experimental results for centre-cracked panels with an example of the crack length $2a = 45mm$ is depicted in Fig. **??** for sheets of Al-foil and LDPE put together with and without adhesion. The latter resulted in the curve independent layers. The differences between the load carrying capacity of the laminate and that of the individual material layers are surprisingly large as described in **?**. The primarily reason to plot Fig. **??**b) with the axis load vs. extension is due to increase of the load carrying capacity is much more obvious. It can also be concluded that the laminate is by far the strongest material and this is not easily conclunded a priori.

4. Procedure for creating SEM images

In order to get the closer understanding of the fracture behavior and process, microscope images were obtained in three steps. In the first step a Leica manufacture mikrotome cutter with a capability to cut $50\mu m$ thin slices along AA and BB direction depicted in Fig. **??**b) was used. The precision of the cutter is well known and especially important is that the cutter is known to leave no damage to the cut slice that may influence the observations. The next step was to cover the specimen with a coating of a few nm of gold particles to increase the resolution and contrast of the picture in the SEM. This was done in a Cressington 108auto sputter coater. The final step was to analyse the prepared test specimen in the SEM, and to create accurate high resolution pictures. The SEM equipment is a Hitachi-Tabletop Microscope, TM-1000 operating at $15keV$. This experimental set-up is available in the Laboratory at Tetra Pak Packaging Solutions AB in Lund.

5. Post-test examination of SEM images

LDPE and Al-foil behave similarly with respect to the overall behavior; localization, geometrical and/or material softening follows after damage initiation, when a centre-crack is introduced in the test specimen Figs. **??** a) and b). The fracture process in the Al-foil is related to how the crystals/grains are built up and in the LDPE there is a combination of how the molecular chains are arranged and how the structural arrangement of the amorphous zones and crystallites are mixed and organised **?**. With respect to fracture both materials display cross sections, perpendicular to the loading direction, in the region close to the crack tip that shows evidence of localised plastic deformation. The post-fracture examination of the Al-foil specimen cross-section shows almost no plastic deformation except for in a small region in the vicinity of the crack plane, as shown in Fig. 5. The upper half of the fractured test specimen is shown in the two figures in Fig. 5 and the section cut is through the thickness direction perpendicular to the loading direction (direction $AA - BB$ in Fig. **??**b)). The LDPE shows both general plastic deformation and localised plastic deformation in a small region close to the crack surface in the vicinty of the crack tip region. In Fig. 5 one observes that the thickness of the LDPE is permanently reduced from $27\mu m$ to around $10\mu m$ except for in the region of localised plastic deformation. The maximum load carrying capacity and the flexibility are very different in the two materials. Nevertheless the two materials act similarly in the cross-sections close to the crack tip. Examination of the edge of the fractured LDPE and Al-foil, using SEM, provides visual evidence to the assumption that fracture occurs through plastic localisation.

Figure 5 shows a fractured laminate consisting of a double-side LDPE coated Al-foil. For this case the matching parts of the crack could be found while an unbroken coating on one side held the specimen together. The image is similar for the case of the Al-foil compared to a single-sided polymer coated Al-foil Fig. 5 and the single Al-foil,

presented Fig. 5. The fractured Al-foil is observed to interact with the surrounding polymer. It is observed that the Al-foil and the LDPE both fail through localised plastic deformation. Localised plastic deformation is also observed to spread into the unbroken LDPE layer.

When a single layer of LDPE is loaded, it normally withstands a rather long extension before breaking, but when laminated with the stiff and strong Al-foil, LDPE is enforced to localised plastic deformation in the region where Al-foil fracture. This phenomena occurs if the adhesion level is sufficently high and hence delamination between the different material layers is not growing. This effect increases the load carrying capacity due to orientation and strain hardening in the locally stretched part and it seems clear that the polymer coating carries load that is many times the load expected at the nominal straining at fracture (see Fig. **??**). The adhesion between the two layers also enforces the dissipation to cover both the fracture of the Al-foil and the LDPE. In-situ tensile testing complemented with microscopic pictures of the fracture zones is needed for increasing the understanding of the micro-mechanisms involved in the sequence of deformation and the fracture process.

6. Localised plastic deformation

The theoretical model (analytical expression) that is used to compute the fracture process is based on an elastic plastic von Mises material model. It is possible that the semicrystalline polymer LDPE has a more complicated behaviour compared to Al-foil, e.g., due to a locking effect that longer molecule chains might cause during excessive straining **?**-**?**. However, considering the tensile test result observed in Fig. **??**, that shows a roughly similar behaviour for both LDPE and Al-foil in the strain region of interest, the same model is used for both materials. The maximum stress occurs at 0.04 to1.2% strain in the Al-foil and from10 to20% strain in the LDPE which is considered to be small to fairly small strains (cf. Fig. **??**).

According to the von Mises elastic perfectly plastic material model, the plastic deformation that is initiated in a uni-axially stretched thin foil immediately localises to a narrow band across the foil. At uniaxial tension, the band forms a straight line that is at a material dependent angle to the pulling direction **?**. The von Mises yield criterion is fulfilled in the band and plastic deformation occurs according to a flow rule. The width of the band is initially close to the original thickness of the foil. During stretching, the band widens and the local thickness is rapidly reduced. When the width has reached twice of its initial width, the thickness is reduced to zero. Simultaneously the load carrying capacity reduces and vanishes when the cross-section disappears.

In the neighbourhood of a crack tip, a consequence of the flow rule is that the strains at first are more or less homogeneously distributed. At this stage the stress field ahead of the crack tip is mostly biaxial which prevents the strain from localising. During increased remote load the crack gets blunted **?** and as this widens the crack tip, the stress parallel with the crack plane is gradually reduced. When this stress is half of the stress perpendicular to the crack plane, the condition for strain localisation is fulfilled, cf. **?**. After this the strains localise to a band continuing ahead from the crack tip as observed by Dugdale **?** who artificially manufactured a blunted crack tip. He observed that the best result was obtained by using cracks with the same width as the thickness of the specimens.

Fig. 1 shows cross-sections with developing bands of localised straining. The structure is a laminate consisting of a stiff layer, Al-foil, bonded to a weak layer, LDPE. The crack is situated in the $x - z$ plane (see Fig. **??**b)). In the band the plastic deformation occurs as a slip line along planes that form a 45°angle to the specimen surfaces. A continuous change of the position of the slip planes leads to the geometries shown in Fig. 1. The adhesion between the two layers is assumed to be strong, hence the interface remains intact in the homogeneously deformed parts of the foil, but not strong enough to prevail in the region between A and B in Fig. 1, where the strains localise. The stiff layer is supposed to deform more or less independently of the behaviour of the weaker layer. Because of that, the localised plastic deformation in the stiff layer introduces large strains in the weak layer that forces it to plastic deformation. Because of these assumptions, the width of the band of localised straining in the weak layer along the interface is the same as the thickness of the stiff layer **?**.

The laminate is subjected to pure tension in the $y-$direction while the stresses in the $z-$direction are expected to be insignificant. Further the variation in the $x-$direction is assumed to be small over distances that are of the order of the laminate thickness. Therefore, plane strain is expected in the $y - z$ plane. Since the plastic strains dominate, the plane strain condition applies directly to the plastic straining, that is inhibited along the band of localised strain. This creates

a tensile stress in the $x-$direction that approaches $\sigma_y/2$, according to the flow rule of von Mises yield condition (cf. **?**). For a single layer, the von Mises effective stress, σ_e, and the yield stress, σ_Y, becomes

$$\sigma_e = \sqrt{\frac{(\sigma_x - \sigma_y)^2}{2}} = \frac{\sqrt{3}}{2}\sigma_y \approx 0.866\sigma_y = \sigma_Y \,, \tag{16}$$

and, thus, the force, F, per unit of length becomes

$$F = \sigma_y t = \frac{2}{\sqrt{3}}\sigma_Y t \approx 1.15\sigma_Y t \,, \tag{17}$$

where t is the actual thickness.

For a laminate where the yield stresses are σ_{YA} in the Al-foil and σ_{YL} in the the LDPE and the original thicknesses are h_A respectively h_L, the corresponding force per unit of length carried by the actual thickness in the localised strain region in a laminate becomes

$$F = \frac{2}{\sqrt{3}}(\sigma_{YA}t_A + \sigma_{YL}t_L) \,, \tag{18}$$

where σ_{YA} and σ_{YL} are the yield stresses of the respective layers, t_A and t_L are the actual Al-foil and LDPE thicknesses in the region of localised strain.

Consider an Al-foil with the original thickness h_A and actual thickness t_A b)). The volume per unit length of the material is supposed to be constant during the plastic deformation. Initially the volume of the plastically deforming segment is $V_o = h_A^2$ (cf. see Fig. 1). After extending the volume the distance δ in the $y-$direction, the volume is readily given by the geometry in Fig. 1b) as $V = (h_A + \delta - t_A)(h_A + t_A)/2 + t_A^2$. The change of volume $V - V_o$ is as follows,

$$V - V_o = (h_A + \delta - t_A)(h_A + t_a)/2 + t_A^2 - h_A^2 = \frac{1}{2}(\delta + t_A - h_A)(t_A + h_A) \,. \tag{19}$$

Thus, $V = V_o$ only have one permissible solution for $t_A = t_A(\delta)$, which according to (19) is,

$$t_A(\delta) = h_A - \delta \,. \tag{20}$$

The slope of the deformed segments is given by the geometric relations in Fig. 1b). Along the surface segments one obtains,

$$\frac{dz}{dy} = \pm\frac{h_A - t_A}{h_A + \delta - t_A} = \pm\frac{1}{2} \,. \tag{21}$$

The deformation of the LDPE layer is modified with regard to the initial slip lines. Because of the influence of the stiffer and harder Al-foil the initial position of the slip lines is the position shown in Fig. 1a). The assumption is that the interface between the laminate layers breaks in the band of localised straining (see Fig. 5) so that there is a simultaneous two-sided thinning of both the Al-foil and the LDPE layer. To maintain continuity across the interface of the extension both layers will give identical width of the localised plastic zone on both sides of the interface (see Fig. 1). When the Al-foil breaks the slip lines meet on the upper part of the LDPE as in Fig. 1c) point C. After this the rate of motion of the point where the sliplines meet is doubled giving a slope of the surface segment $dz/dy = \pm 1$. To maintain constant volume rate along the simultaneously created surface segment on the lower part of the LDPE, the inclination of the created surface should be $dz/dy = \pm 1/3$, which is obtained by using geometrical considerations. The moment the LDPE and thereby the entire structure fractures is displayed in Fig. 1d).

The surface profiles shown in Figs. 5, 5, 5 and **??** give confidence to the assumption that the fracture occurs through localised plastic straining. In Fig. **??** the slope 1:2 that is included in the SEM image shows a fair fit to the image of the fractured Al-foil. The correspondingly included theoretical profile for the LDPE is also reasonably similar to the experimental result. One has to consider that the LDPE is a soft and flexible material and the fractured cross-section may have been slightly deformed during the specimen cutting, preparation and mounting which may partly account for the discrepancies between the theoretical and the experimental results.

Local plastic deformation leading to complete separation of a metallic foil of Al-foil was observed by Dugdale **?** and the same for other metallic materials by several other investigators after him **?**. The essence of the observation is that the fracture process of thin foils of many different materials is essentially a purely plastic process, that depends on the elastic-plastic material properties and the layer thickness. The lack of stress constraint because of insignificant stress across the plane of the foil causes the foil to deform plastically at a stress on the level of the yield stress. That prevents the development of the high stress that is required for cleavage fracture or initiation of voids for ductile fracture. The plastic deformation leads to purely plastic failure before the fracture toughness of the material is reached. This means that the macroscopically observed critical stress intensity factor is, as opposed to the fracture toughness, not a material property.

As observed in Fig. 5 the cross-section is thinned to vanishing thickness as an effect of the plastic deformation for both the Al-foil and the LDPE. Under these circumstances, it seems reasonable to assume that the final breaking of the cross-section has very little effect on the process as a whole. The suggested type of the fracture process based on pure plastic deformation depending on a strong coupling between the individual layers of laminates, has been suggested by **?**.

For both layers the geometrical relation between the layer thickness and the extension δ of the region becomes

The force per unit of length along the $x-$direction according to (18) becomes

The relation to the spatial coordinate ahead of the crack tip requires a solution of linearly elastic problem for the body. Such a solution can be achieved analytically using an integral equation method as in **?** or by application of a numerical finite element method. The cohesive stress is then applied as boundary conditions of a Robin type. Figure **??** shows the cohesive stress as a function of the displacement according to (**??**). The kink connecting the two linear segments indicates when the thinner foil is discontinued. Graf i sigma

7. A fracture mechanical model

Consider a laminated panel containing a centre-crack. A coordinate system is attached to one of the crack tips as shown in Fig. **??**. the crack tip, give the coordinates of the panel as $|x + a| \leq W$, $|y| \leq H$ and $|z| \leq h/2$, where $h = h_A + h_L$. The initial position of the crack is $|x + a| \leq a$, $y = 0$ and $|z| \leq h/2$ (see a picture of the panel in Fig. **??**). A cohesive stress $\sigma_D(\delta) = F(\delta)/h$, where δ is the discontinous displacement between the upper and lower surfaces of the region $0 < x \leq \rho$, $y = 0$ and $|z| \leq h/2$, cf. Fig. **??**. The cohesive force, $F(\delta)$, is given according to Fig. **??**. The developing region of localised strain is observed in the $y - z$ plane in Fig. **??**b).

By considering that the in-plane strains ϵ_x and ϵ_y are equal in both layers one may replace the individual elastic parameters with an equivalent modulus E and an equivalent Poisson's ratio, ν, that then become applicable to the laminated structure as if it was a homogeneous material. The equivalent cohesive stress is as it is given by (**??**).

The mathematical solution for arbitrary cohesive stresses may be solved using Muskhelishvili's method **?**. The obtained integral equation may be solved using an iterative method because of the mixed boundary condition in the cohesive zone, where $F = F(\delta)$, cf. **?**. At small scale yielding, i.e. when ρ is much shorter than the length of the crack and the distance to the traction free boundary, the critical value of the J-integral **?** is directly given by the work required to break the foil **?**. The following relation, readily computed from evolving geometry of the cross-section, gives the critical value of the J-integral, J_c, as, cf. **?**,

Table 2 shows the calculated values for the Al-foil, the LDPE and the laminate. The toughness J as calculated from (**??**). Also the critical J:s of the individual foils are computed using (**??**) by putting the thickness of the respective counterpart to zero.

To compute the small scale yielding result for the limiting stress depending on the crack length the result by **?** is used. The following expression is provided when the LEFM fails to describe the experimental result for the short crack lengths the following strip yield model is used, cf. **?**. The following gives the critical stress σ_c at initiation of crack growth

$$\sigma_c = \sqrt{\frac{J_c E}{2\pi a}} \frac{1}{\phi\left(\frac{a}{W}\right)} = \sqrt{\frac{\left(\sigma_{yA} h_A + \sigma_{yL} h_L\right) E}{2\sqrt{3}\pi a}} \frac{1}{\phi\left(\frac{a}{W}\right)}, \tag{22}$$

where

$$\phi\left(\frac{a}{W}\right) = \frac{1 - 0.025(\frac{a}{W})^2 + 0.06(\frac{a}{W})^4}{\sqrt{\cos[\frac{\pi}{2}\frac{a}{W}]}}, \tag{23}$$

cf. **?**. The result has been included in Fig. **??**. The results obtained from the experimental data are the normalised stress at break values versus normalised crack lengths, shown in Fig. **??**.

8. Results and Discussion

At post-fracture examination with the aid of SEM micrographs, practically no fracture surface could be observed. This was observed for single layers of Al-foil and the LDPE polymer both separate and bonded together to a laminate. The cross-sections are thinned to vanishing thicknesses as an effect of the plastic deformation for both the Al-foil and the LDPE. Under these circumstances, it seems reasonable to assume that the final breaking of the cross-section is obsolete or, at least, that it has very little effect on the fracture process as a whole. Therefore the governing fracture process is based on pure plastic deformation and depending on a strong coupling between the individual layers of the laminates.

The adhesion between the packaging material layers, in this study Al-foil and LDPE, significantly increases peak load and fracture toughness in a laminate. An LDPE polymer film that alone withstands a rather long extension before breaking shifts, in a laminate, to localised plastic deformation close to the crack tip. The reason observed is that the stiffer Al-foil enforces localised plastic deformation and fracture in the polymer at a small nominal strain. This result in increased load carrying capacity of the polymer locally by around 4 to 5 times (see Fig. **??**).

The mechanical behaviour of the laminate also forces both the Al-foil and the polymer to fracture simultaneously which increases the fracture toughness many times as compared to the added toughnesses of the individual layers.

A slip line model is presented for the localised plastic deformation. The model can be used to predict the mechanical behaviour of the LDPE and the Al-foil.

The slip line model is incorporated in a strip yield model that is successfully used to predict the behaviour of the individual layers, cf. Fig. **??**.

Fig. **??** shows the local behaviour perpendicular to the loading direction in the vicinity of the fractured surface where the crack has grown and where localised plasticity driven fracture process has occurred.

In-situ experimental tests with complementary SEM-micrographs of the plastic strain localization during the course of stretching is needed to conform the theoretical conclusions that has been concluded in this work, both for one side and two side laminated Al-foil??? surface cracks and defects arrest in the Al-foil and hence is the material behavior reinforced and observed to increase in loading capacity when laminated. Two-sided lamination is reinforcing both sides hence the material is perceived as a stronger material compared to testing single material layer. LDPE is also forced to localize if the adhesion level is sufficient to not govern delamination in-between the material layers. If the polymer is observed to strain-hardening the load curve can be improved/increased significantly. Figuren 6 ger support fr att det r ren plasticitet. Man ser ingen brottyta. Det ar viktigt att det ar enbart plasticitet. Rawdata fr LDPE $a = 45mm$? Behver vi sigma_break? Det r vl primrt flytspnningen vi bygger antagandenda samt slutsaterna kring?

Should we include the fomula to calculate $E_{laminate}$?? Young's modulus can be accurately estimated for the laminate by the theory of the elastic mechanics of applicable in composite materials described in [15] (Warren, R., Composite Materials. Inst. for Metalliska Konstruktionsmaterial, Sweden, 1986/87. or Staab, George H., Laminar Composites. Butterworth- Heinemann, 1999) Here, Ei, i and ti are Young's modulus, Poisson's ratio and the thickness of layer i, respectively.

9. Conclusions

Adopting a slip-line theory with a resulting 1:2 inclination of the fractured cross sections seems reasonable for individual Al-foil but not explaining all the governing pheonoma in LDPE.

This theory is also applicable on cross sections created when fracturing laminated Al-foil with one- and two-sided laminated LDPE.

LEFM is valid when 2a¡ x mm and by this behavior togheter with LEFM an analytical expression has been derived for prediction of critical load of both individual layers and a packaging laminate consisting of one-side laminated Al-foil with LDPE. This expression can be used when the plastic region is much smaller thatn the crack length...

Acknowledgements

Acknowledgements and Reference heading should be left justified, bold, with the first letter capitalized but have no numbers. Text below continues as normal.

References

Clark, T., Woodley, R., De Halas, D., 1962. Gas-Graphite Systems, in "*Nuclear Graphite*". In: Nightingale, R. (Ed.). Academic Press, New York, pp. 387.

Deal, B., Grove, A., 1965. General Relationship for the Thermal Oxidation of Silicon. Journal of Applied Physics 36, 37–70.

Deep-Burn Project: Annual Report for 2009, Idaho National Laboratory, Sept. 2009.

Fachinger, J., den Exter, M., Grambow, B., Holgerson, S., Landesmann, C., Titov, M., Podruhzina, T., 2004. "Behavior of spent HTR fuel elements in aquatic phases of repository host rock formations," 2nd International Topical Meeting on High Temperature Reactor Technology. Beijing, China, paper #B08.

Fachinger, J., 2006. Behavior of HTR Fuel Elements in Aquatic Phases of Repository Host Rock Formations. Nuclear Engineering & Design 236, 54.

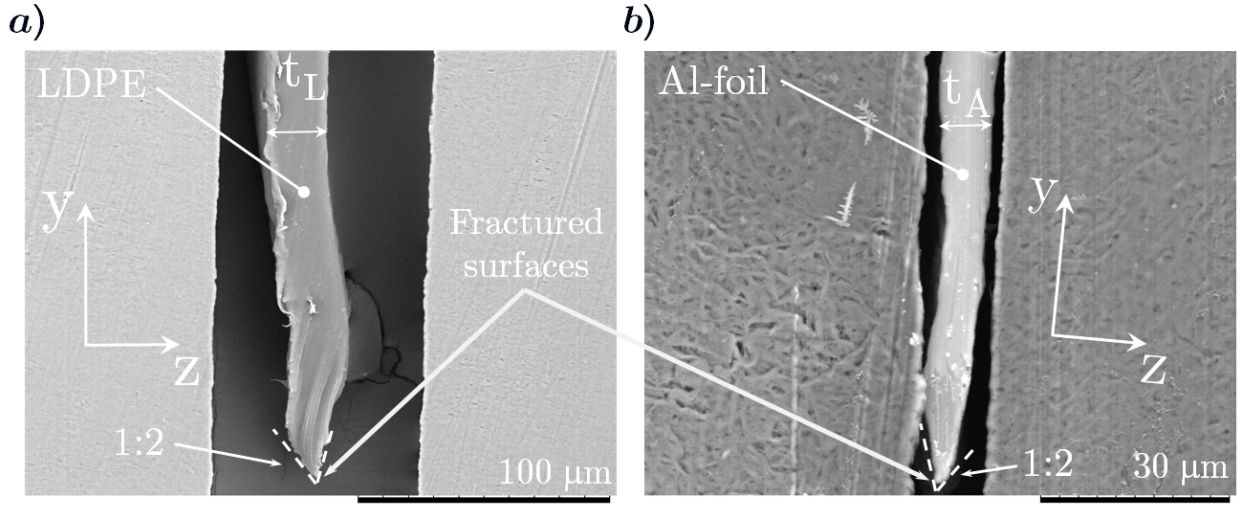
a)
b)
LDPE
t_L
y
z
Fractured surfaces
1:2
100 µm
Al-foil
t_A
y
z
1:2
30 µm

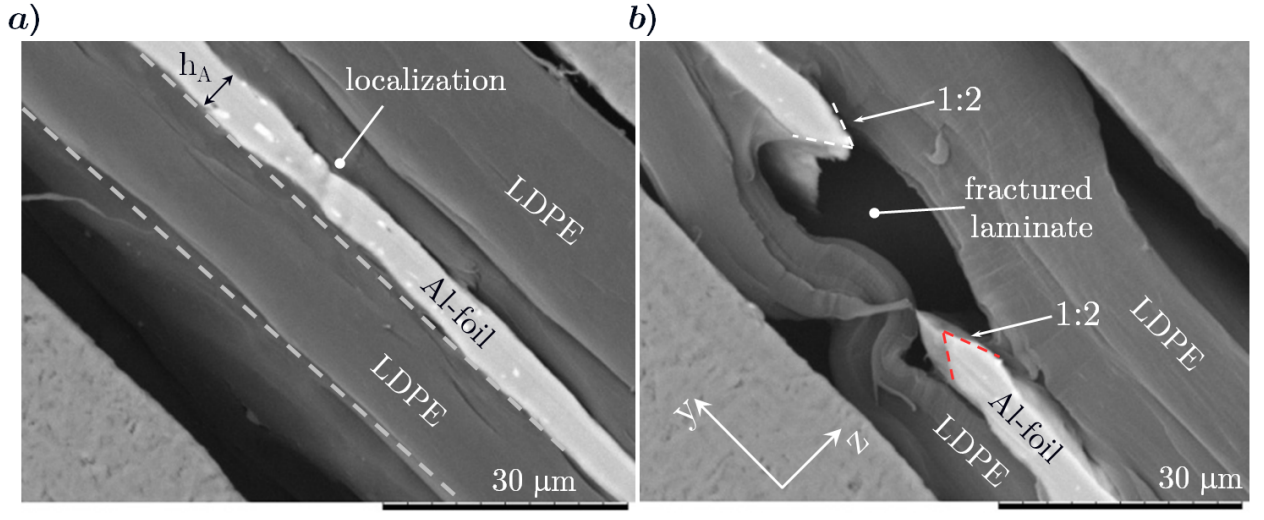
a)
b)
h_A
localization
LDPE
Al-foil
LDPE
30 µm
1:2
fractured laminate
1:2
LDPE
y
z
Al-foil
LDPE
30 µm

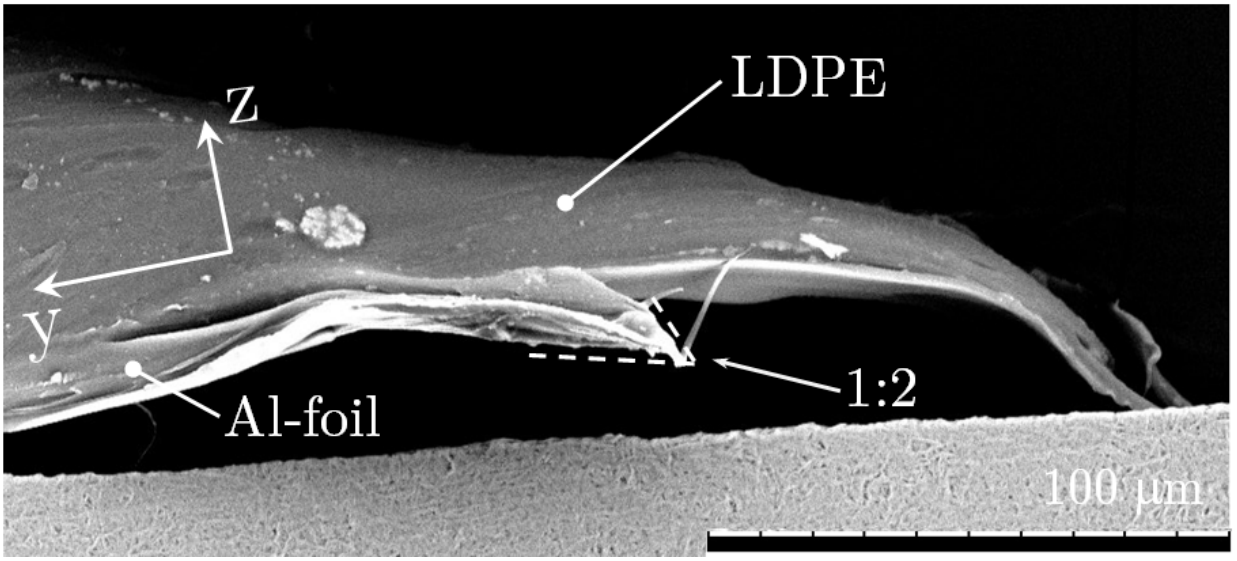

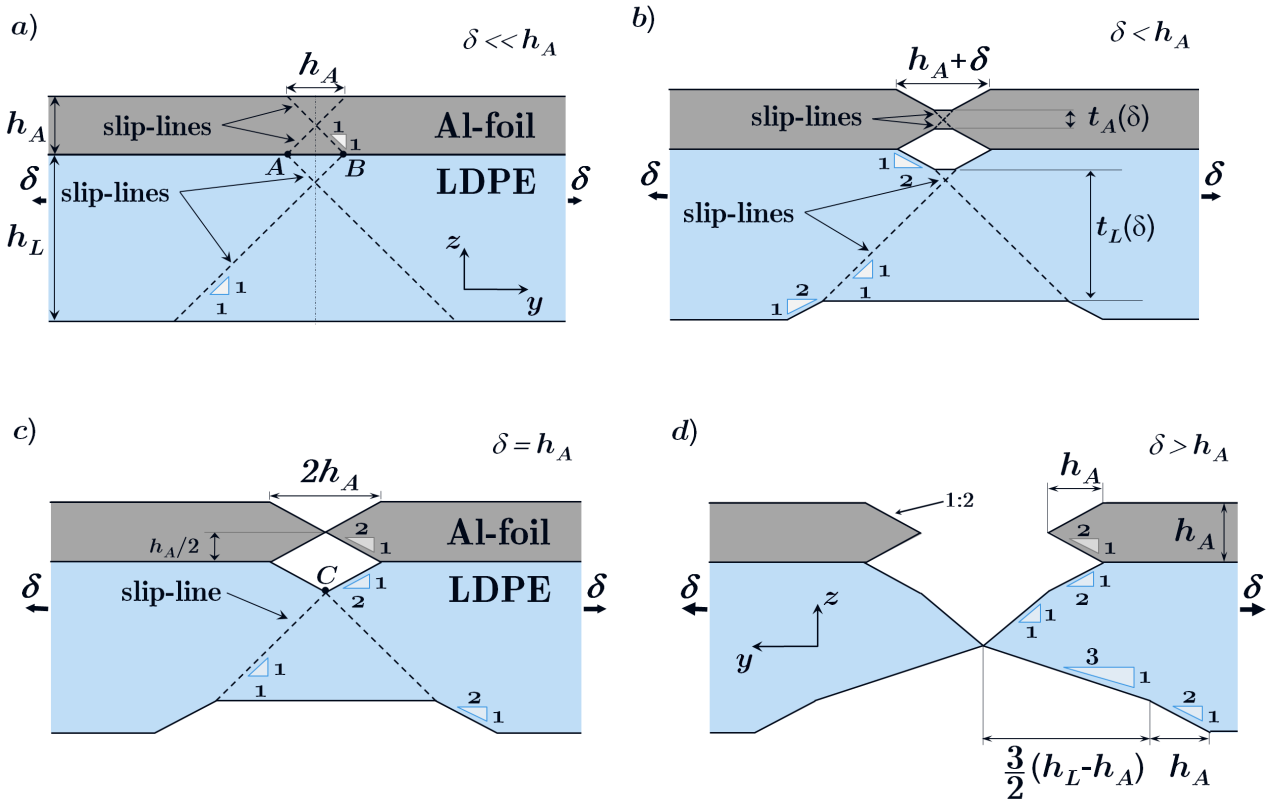

Fig. 1. Specimen cross-section and slip lines of the two layers of the laminate with a broken interface in the region of localised plastic deformation; a), b), c) and d) show the separated layers defining the reduction of their cross-sections during deformation and damage process. The materials are stretched in *y*-direction.